Electrocorticography reveals the temporal dynamics of posterior parietal cortical activity during recognition memory decisions

Alex Gonzalez[a], J. Benjamin Hutchinson[b], Melina R. Uncapher[b], Janice Chen[b], Karen F. LaRocque[b], Brett L. Foster[c], Vinitha Rangarajan[c], Josef Parvizi[c,d], and Anthony D. Wagner[b,d,1]

[a]Department of Electrical Engineering, Stanford University, Stanford, CA 94305; [b]Department of Psychology, Stanford University, Stanford, CA 94305; [c]Department of Neurology and Neurological Sciences, Stanford University, Stanford, CA 94305; and [d]Neurosciences Program, Stanford University, Stanford, CA 94305

Edited by Larry R. Squire, Veterans Affairs San Diego Healthcare System, San Diego, CA, and approved July 22, 2015 (received for review June 3, 2015)

Theories of the neurobiology of episodic memory predominantly focus on the contributions of medial temporal lobe structures, based on extensive lesion, electrophysiological, and imaging evidence. Against this backdrop, functional neuroimaging data have unexpectedly implicated left posterior parietal cortex (PPC) in episodic retrieval, revealing distinct activation patterns in PPC subregions as humans make memory-related decisions. To date, theorizing about the functional contributions of PPC has been hampered by the absence of information about the temporal dynamics of PPC activity as retrieval unfolds. Here, we leveraged electrocorticography to examine the temporal profile of high gamma power (HGP) in dorsal PPC subregions as participants made old/new recognition memory decisions. A double dissociation in memory-related HGP was observed, with activity in left intraparietal sulcus (IPS) and left superior parietal lobule (SPL) differing in time and sign for recognized old items (Hits) and correctly rejected novel items (CRs). Specifically, HGP in left IPS increased for Hits 300–700 ms poststimulus onset, and decayed to baseline ∼200 ms preresponse. By contrast, HGP in left SPL increased for CRs early after stimulus onset (200–300 ms) and late in the memory decision (from 700 ms to response). These memory-related effects were unique to left PPC, as they were not observed in right PPC. Finally, memory-related HGP in left IPS and SPL was sufficiently reliable to enable brain-based decoding of the participant's memory state at the single-trial level, using multivariate pattern classification. Collectively, these data provide insights into left PPC temporal dynamics as humans make recognition memory decisions.

intracranial EEG | declarative memory | decision making | multivariate pattern analysis | ECoG

The ability to remember past events—episodic memory—is known to critically depend on medial temporal lobe (MTL) structures (1, 2) and their interaction with prefrontal cortex (3). Neuroimaging studies of humans making memory-based decisions, although advancing understanding of MTL and prefrontal mnemonic function (4–8), consistently and unexpectedly demonstrate that activity in left lateral posterior parietal cortex (PPC) also varies with episodic memory outcomes (9–14). In particular, functional MRI (fMRI) data reveal dissociable effects of memory on activity in left intraparietal sulcus (IPS), superior parietal lobule (SPL), and angular gyrus (AG), wherein activity tracks perceived memory strength, retrieval decision uncertainty, and episodic recollection, respectively (9–14). For example, during recognition memory decisions, activity in left lateral IPS is greater during higher confidence hits and monotonically decreases across lower confidence hits to lower confidence correct rejections (CRs) to higher confidence CRs (15–17). By contrast, activity in left SPL is greater during lower confidence recognition decisions (for both hits and correct rejections) relative to higher confidence decisions (11, 16, 17).

Studies of patients with PPC lesions demonstrate a complex pattern of effects on memory, with performance spared on some measures of episodic memory, but impaired as measured by retrieval confidence, memory for source details, and cued recall (18–23). For example, a recent study of two patients with bilateral IPS lesions revealed unimpaired recognition memory accuracy, but a reduction in high confidence hits and false alarms relative to matched controls (22). Importantly, this decline in high confidence recognition decisions was only observed for items perceived as old, and not for items perceived as novel. As with fMRI measures of left lateral IPS activity, these lesion data suggest that the role of IPS in memory varies as a function of whether the test probe is perceived as old or new.

The role of lateral PPC in episodic retrieval is posited to relate to broader (i.e., nonmnemonic) functions. Extant evidence indicates that dorsal PPC is involved in other cognitive domains, such as perceptual decision making (24–28). For example, human fMRI studies of two-choice perceptual decisions have demonstrated that IPS activity tracks the strength of perceptual evidence (24, 25), independent of response modality (25). A mechanistic interpretation of such activity is that IPS neurons act as evidence accumulators, with a distinct population of IPS neurons accumulating evidence toward each of the two decision bounds. When the evidence reaches one of the bounds, a perceptual decision it thought to be reached. Such results motivated the hypothesis that left IPS might serve as a mnemonic accumulator during old/new recognition decisions (9, 16).

Significance

Over the past decade, human posterior parietal cortex (PPC) has been unexpectedly implicated in remembering and memory-related decision making. Functional neuroimaging indicates that memory-related responses differ across PPC, and patients with PPC lesions show subtle to significant changes in memory behavior. These surprising observations have motivated novel theorizing, yet current understanding of PPC contributions to memory is limited by the absence of temporal information about activity in PPC subregions as retrieval decisions unfold. In this study, recordings from the human brain show for the first time that distinct temporal and functional profiles of activity are present in PPC subregions as participants make recognition memory decisions. These new findings inform theories of parietal functional contributions to memory, decision making, and attention.

Author contributions: J.B.H., M.R.U., and A.D.W. designed research; A.G., J.B.H., J.C., K.F.L., B.L.F., V.R., and J.P. performed research; A.G. and M.R.U. analyzed data; and A.G. and A.D.W. wrote the paper.

The authors declare no conflict of interest.

This article is a PNAS Direct Submission.

[1]To whom correspondence should be addressed. Email: awagner@stanford.edu.

This article contains supporting information online at www.pnas.org/lookup/suppl/doi:10.1073/pnas.1510749112/-/DCSupplemental.

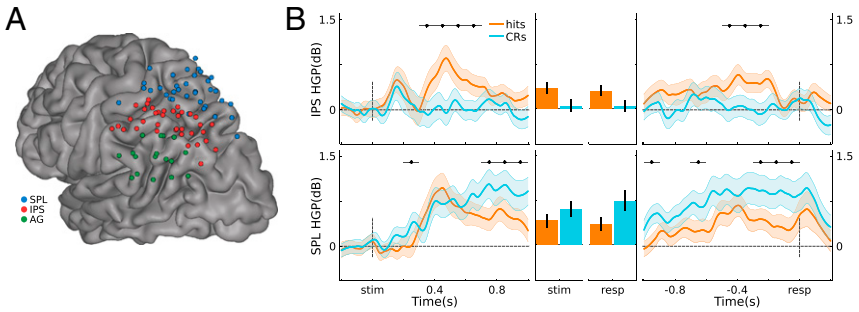

Fig. 1. (*A*) Electrode coverage in left lateral PPC across participants. (*B*) Stimulus-locked (*Left*) and response-locked (*Right*) HGP time courses for Hits and CRs, for the IPS and SPL electrodes. Gray bars indicate significant differences between Hits and CRs ($P < 0.05$*; Bonferroni corrected; error bars, SEM). (*Middle*) Time-averaged HGP in IPS and SPL.

By contrast, SPL is a core component of the dorsal fronto-parietal network that implements top-down visual attention (29, 30). Parallel lines of work in the memory and perception literatures demonstrate that left SPL activity is greater during uncertain memory decisions (17) and uncertain perceptual decisions (31). Such findings suggest that decision uncertainty, be it in the mnemonic or perceptual realm, results in increased engagement of top-down visual attention to driving inputs (17).

Although the preceding suggests a possible functional differentiation between IPS and SPL during decision making, an alternative account posits that IPS and SPL activity during retrieval reflects a common attention function (11). In this view, dorsal PPC retrieval activity is seen as a reflection of top-down attention, acting to maintain retrieval goals and to monitor memory signals that presumably emerge from MTL computations. One challenge for this perspective is the distinct patterns of fMRI blood oxygen level-dependent (BOLD) signal in left IPS and SPL during episodic retrieval (16, 17, 32).

Theorizing about the distinct memory-related response profiles in dorsal PPC subregions observed with fMRI—that is, in IPS and SPL—has been hampered by the absence of precise information about the temporal dynamics of lateral parietal activity. Although scalp-recorded event-related potentials (ERPs) demonstrate a differential positivity over left parietal cortex as a function of recognition memory (hits > CRs, ~400–800 ms postretrieval cue onset) (33), the anatomical source(s) of this parietal "old/new" effect and its relation to the multiple memory-related PPC effects observed with fMRI remain unknown. A recent effort to use simultaneous EEG–fMRI to advance understanding of the temporal profile of parietal activity during retrieval did not reveal a link between ERP and fMRI BOLD effects in any lateral parietal region (34). Importantly, the hypothesis that IPS and SPL subserve distinct computations predicts that these subregions will display different temporal response patterns during memory-based decisions; these patterns promise to directly inform hypotheses about their functional roles. More broadly, understanding the temporal profile of responses in these subregions of PPC during decision making may inform theories of dorsal PPC function across cognitive domains, including perceptual decision making and attention.

A correlate of fMRI BOLD activity is provided by the high-frequency range of local field potentials (LFPs) (35–38), which reflects local population activity (39–41), providing a means to specify and dissociate the temporal dynamics of memory effects in specific PPC regions. Accordingly, we used electrocorticography (ECoG) to directly record cortical LFPs from human left IPS and SPL while participants made recognition memory decisions. During the encoding phase, participants viewed a series of individually presented nouns, making abstract/concrete judgments on each. Subsequently, participants made old/new recognition judgments about test items, half studied and half novel (Fig. S1; see *Materials and Methods*). LFPs were recorded in eight participants (Fig. S2 and Table S1) with medication-resistant epilepsy, using subdural grids or strips implanted in left PPC (five participants) or right PPC (control data; three participants).

Results

Univariate Analyses. Using gross anatomical landmarks, electrodes were localized to left IPS or SPL (Fig. 1*A*, *SI Text*, and Fig. S2; three participants also had electrodes in left AG). To test for stimulus-locked memory-related changes during retrieval, we quantified the difference in high gamma power (HGP; 80–180 Hz) between Hits (old items correctly recognized with high confidence) and CRs (novel items correctly rejected with high confidence) using the Mann–Whitney U statistic across 100-ms time bins per channel. This resulted in 10 bins ranging from the beginning of retrieval cue presentation to 1 s postretrieval cue onset. The effect of Memory (U score on Hits vs. CRs) on stimulus-locked HGP showed a Time × Region (IPS, SPL) interaction ($F_{(9,621)} = 2.32$, $P = 0.014$), indicating that memory-related activity differentially varied across time in left IPS and SPL (Fig. 1*B*). Specifically, in left IPS channels, Memory varied across Time ($F_{(9,315)} = 6.58$, $P = 1.3\text{e-}8$), revealing greater HGP during Hits than CRs from 300 ms to 700 ms ($ts_{(35)} > 3.78$, $ps < 0.05$*, with the "*" indicating Bonferroni corrected; Fig. 1*B*, *Left*). Strikingly, during these windows, HGP on CR trials did not differ from baseline ($ts_{(35)} < 1.75$, $ps > 0.05$). Left SPL channels also exhibited an effect of Memory that varied across Time ($F_{(9,306)} = 6.97$, $P = 3.7\text{e-}9$), but, contrary to left IPS, HGP was greater during CRs than Hits both early (200–300 ms; $t_{(34)} = 3.33$, $ps < 0.05$*) and late (700–1,000 ms; $ts_{(34)} > 3.04$, $ps < 0.05$*). As such, memory-related HGP in left IPS and SPL differed in time and sign over the course of making decisions about items that were correctly recognized as old or new. Importantly, these results held when analyses were performed across participants rather than channels (*SI Text* and Figs. S3–S5), and Memory × Region dissociations were evident even when averaging across time (Fig. 1*B*).

Further insights into the processes subserved by left IPS and SPL can be obtained by analyzing response-locked data. Here, the analysis window ranged from 1 s preresponse to 200 ms postresponse, with HGP data binned into 100-ms bins for a total of 12 bins; the effects of memory (Hits vs. CRs) were quantified by the U score. Left IPS showed Memory effects that varied across Time ($F_{(11,385)} = 4.44$, $P = 2.6\text{e-}6$), whereas SPL showed a strong main effect of Memory but no interaction with Time ($t_{(34)} = 3.94$, $P = 4.0\text{e-}4$ and $F_{(11,374)} = 1.47$, $P = 0.14$, respectively). There was no Time × Region interaction for the response-locked analyses ($F_{(11,759)} = 1.56$, $P = 0.11$; but see *SI Text* for subject-level analyses that revealed a Time × Region interaction). These effects are shown on Fig. 1*B*, *Right*, with IPS and SPL clearly showing opposite effects of Memory. Left IPS channels showed greater HGP for Hits than CRs in a preresponse time window (500 m to 200 ms; $ts_{(35)} > 3.40$, $ps < 0.05$*), with activity for Hits appearing to fall to baseline ~200 ms preresponse; HGP for CRs did not deviate from baseline before response ($ts_{(35)} < 1.64$, $ps > 0.11$). By contrast, left SPL channels showed above-baseline HGP for CRs throughout the preresponse period ($ts_{(34)} > 3.39$, $ps < 0.05$*), with HGP for CRs being greater than for Hits both early (1,000–900 ms and 700–600 ms; $ts_{(34)} > 3.08$, $ps < 0.05$*) and from 300 ms preresponse up to the response ($ts_{(34)} > 3.27$, $ps < 0.05$*). Again, these results were also evident after averaging across Time (Fig. 1*B*). See *SI Text* and Fig. S6 for the corresponding analyses in AG.

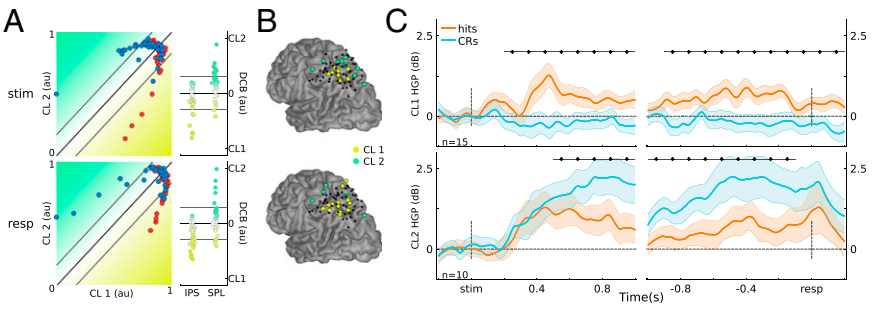

Fig. 2. Clustering results. (*A*) (*Left*) Scatter plot of normalized electrode distance to each cluster. (*Right*) Distance to decision boundary (DCB). Gray lines indicate threshold of 1 SD. (*B*) Electrode grouping for threshold clusters. (*C*) Merged CL1 and CL2 HGP time courses ($P < 0.05$*; Bonferroni corrected; error bars, SEM); au, arbitrary units.

The left laterality of memory-related activity in PPC has been reported extensively in the literature; hence we did not expect to observe similar effects in right PPC. A control group of three patients with electrode coverage in the right lateral PPC performed the experiment (see Fig. S2 for electrode coverage, Fig. S7 for retrieval time courses, and *SI Text* for additional analyses). Qualitatively, the time courses for Hits and CRs in right PPC did not differ and did not resemble those in left PPC. Quantitatively, we tested the HGP Memory U score in right PPC. On stimulus-locked data, we observed no effect of memory across Time in right IPS ($F_{(9,198)} = 0.65$, $P = 0.75$) or right SPL ($F_{(9,117)} = 1.01$, $P = 0.44$). In addition, the Time × Region (right IPS, right SPL) interaction was not significant ($F_{(9,315)} = 0.48$, $P = 0.89$). Finally, comparison of effects in the right and left hemispheres revealed a significant Time × Hemisphere interaction ($F_{(9,936)} = 2.23$, $P = 0.02$). These observations indicate that stimulus-locked memory effects and memory-related regional dynamics were specific to left PPC. For response-locked data, again we observed no effect of memory across Time in right SPL ($F_{(11,143)} = 1.67$, $P = 0.09$). Right IPS did show a Time-varying effect of memory ($F_{(11,242)} = 3.07$, $P = 7.1e\text{-}4$), but the only significant time windows were postresponse (CRs > Hits, $P < 0.05$*; Fig. S7), with no hint of the signed preresponse memory effect observed in left IPS. As with stimulus-locked analyses, the Time × Region (right IPS, right SPL) interaction was not significant ($F_{(11,385)} = 1.17$, $P = 0.31$), and there was a significant Time × Hemisphere interaction ($F_{(11,1144)} = 2.04$, $P = 0.02$). Thus, although asymmetric effects of distal epileptic discharges are difficult to definitively rule out, these results support the a priori prediction that retrieval effects on HGP would be predominantly left-lateralized.

Functional Grouping of Electrodes. The preceding analyses used anatomy-based electrode groupings to examine IPS and SPL memory effects. An alternative approach is to examine how the data cluster according to their activity patterns using clustering analyses. We used a K-means clustering approach to provide an independent test of whether memory-related HGP functional responses exhibit anatomical dissociations. With K = 2, we assigned cluster 1 (CL1) as the IPS cluster and cluster 2 (CL2) as the SPL cluster. This analysis yielded substantial overlap between the resulting cluster groupings and the anatomical channel labels (number of overlapping labels/total labels: stimulus-locked 51/71, response-locked 52/71; Fig. 2*A*). Moreover, the average certainty for cluster membership (distance to the cluster decision boundary; see *Materials and Methods*) was higher for correctly labeled channels (coincident cluster grouping to anatomical label) than incorrectly labeled channels (stimulus-locked: M correct = 0.11, M incorrect = 0.05, $t_{(69)} = 2.76 < 0.01$; response-locked: M correct = 0.10, M incorrect = 0.06, $t_{(69)} = 2.04$, $P = 0.05$).

Next, we formed a unified cluster representation by first selecting channels that had high cluster membership: ≥1 SD away from the decision boundary (Fig. 2*A*, *Right*; stimulus-locked: 8 for CL1, 9 for CL2; response-locked: 14 for CL1, 5 for CL2). The selected channels can be thought as having high-confidence membership in a given cluster. Again, the resulting clusters strongly coincided with left IPS (CL1) and SPL (CL2) (Fig. 2*B*). Channels showing high cluster membership for both clustering analyses (stimulus- and response-locked) were merged, yielding 15 electrodes in CL1 and 10 in CL2.

Critically, the memory-related effects on HGP in CL1 and CL2 replicated those observed using anatomy-based groupings (Fig. 2*C* and Figs. S8 and S9). Importantly, the two resulting unified clusters did not contain overlapping electrodes (Fig. 2*B*), and each participant was represented in both merged clusters (CL1: S1 = 2, S2 = 4, S3 = 1, S4 = 7, S5 = 1; CL2: S1 = 2, S3 = 2, S4 = 4, S5 = 2). Fig. 2*C* shows the HGP time courses for the merged clusters. Figs. S8 and S9 show the HGP time courses for the separate clusters using K-means on the stimulus-locked and on the response-locked data, respectively. The key observation here is that the obtained stimulus-locked and response-locked channel clusters are consistent with the anatomically based electrode groupings.

Our decision to use K = 2 for the cluster-based analysis was motivated by the functional neuroimaging literature, which has revealed at least two distinct memory-related BOLD responses in dorsal PPC. Note that, by using K = 2 and selecting only the channels with strong cluster membership, we effectively created a third "noise" channels cluster (Fig. 2 *A* and *B*). A post hoc clustering analysis using K = 3 and K = 4 was performed to investigate the possibility of functional subclusters within the regions of interest. Fig. S10 shows the results of analyzing the stimulus-locked and response-locked data with K = 3 and K = 4. All analyses yielded at least one dorsal (SPL) and one ventral (IPS) electrode cluster, coinciding with our initial choice of K = 2, and the original anatomically based groupings. No congruent subclusters emerged from these analyses.

Decoding Analyses. To assess the reliability of memory-related information contained in individual left PPC channels within our regions of interest, we examined the discriminability between Hits and CRs on a single-trial basis using HGP time bins as features. Left IPS and SPL channels both enabled above-chance decoding of Hits and CRs using stimulus-locked (IPS M = 53%, SPL M = 54%; $P < 0.05$) and response-locked HGP (IPS M = 53%, SPL M = 56%, $P < 0.05$; Fig. 3*A*; see *SI Text* for full statistics).

Next, we pooled channels within each PPC region to form a spatiotemporal feature set for the decoder, allowing us to examine effects at the participant level. Across participants, average accuracy for stimulus-locked data from left IPS was 57% and from left SPL was 65% ($P < 0.05$); for the response-locked data, IPS accuracy was 57% and SPL was 70% ($P < 0.05$; Fig. 3*B*). Finally, we pooled across both left IPS and SPL electrodes to obtain a single score of memory decoding performance for each participant. For stimulus-locked analysis, we obtained a mean classification rate of 65% (S1 = 64%, S3 = 64%, S4 = 75%, S5 = 58%; $P < 0.05$). For response-locked data, the mean classification rate was 69% (S1 = 71%, S3 = 56%, S4 = 71%, S5 = 78%; $P < 0.05$). Overall, these analyses demonstrate that memory-related information is contained at the individual channel level in IPS and SPL and, furthermore, that we can use spatiotemporal information to decode Hits vs. CRs at the participant level.

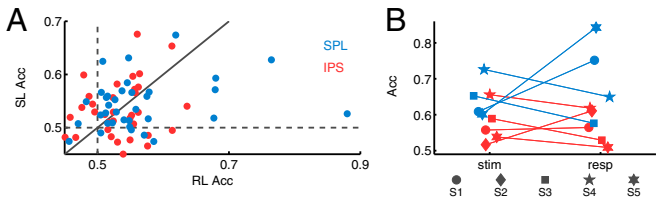

Fig. 3. (*A*) Scatter plot of channel classification accuracy for stimulus-locked (SL) and response-locked (RL) data. Acc, decoding accuracy. (*B*) Subject-level accuracy by region and lock condition. All classification accuracies based on Hits vs. CRs.

Discussion

The present findings provide three insights into PPC temporal dynamics during memory-based decisions. First, HGP (80–180 Hz) in IPS channels was higher for correctly recognized old items (Hits) than correctly rejected novel items (CRs), starting ∼300 ms poststimulus onset. Response-locked analyses furthered revealed that HGP for Hits decayed to baseline ∼200 ms preresponse. Notably, HGP for CRs did not differ from baseline during the retrieval and decision period. Second, HGP in the SPL showed a distinct temporal profile with an inverse sign, with activity greater for CRs than Hits. Specifically, HGP for CRs was greater than for Hits early (200–300 ms poststimulus), was then similarly elevated above baseline for CRs and Hits (300–700 ms), and, finally, was greater again for CRs than Hits starting ∼700 ms poststimulus presentation and lasting until after a response was made. These differences produced a significant Time × Region interaction, even when analyzed across participants. Moreover, this functional dissociation between memory-related HGP temporal dynamics in left IPS and SPL was also detected when using a clustering procedure. Third, the separable temporal patterns of HGP for Hits and CRs in left IPS and SPL were reliable on a trial-by-trial basis, as measured by the above-chance memory decoding performance achieved by a trained multivariate pattern classifier, at both the channel and participant level.

Extant fMRI data indicate that left IPS activity is greater for hits than CRs (9, 12, 42), with IPS activity systematically tracking perceived memory strength (high-confidence hits > low-confidence hits > low-confidence CRs > high-confidence CRs) (17). Recent lesion data also implicate IPS in subjective assessments of memory strength or signed decision confidence (22). In particular, two patients with IPS lesions, although demonstrating intact recognition memory accuracy, recognized fewer items (hits and false alarms) with high confidence than did matched controls. By contrast, the patients' confidence in novel decisions (CRs and misses) was comparable to controls. As such, both fMRI BOLD activity in left IPS during recognition decisions and the effects of IPS lesions on decision confidence are similarly signed, with left IPS appearing to be differentially engaged/necessary for high-confidence old responses.

Consistent with, and substantially extending, these fMRI and lesion findings, our direct electrophysiological data demonstrated greater left IPS HGP for Hits than CRs. Furthermore, HGP for CRs did not differ from baseline, which converges with the null effect of IPS lesions on memory confidence for items perceived as novel. Because the memory performance of the patients in our study was high, the patients primarily made high-confidence old and high-confidence new responses. Future studies are needed to determine whether HGP in left IPS linearly varies with perceived memory strength, as observed with BOLD fMRI.

In addition to revealing a selective HGP increase to Hits in left IPS, the present data also provide evidence about the temporal dynamics and functional role of IPS activity during recognition decisions. Functional MRI studies of two-choice perceptual decisions in humans have demonstrated that IPS activity tracks perceptual evidence strength (24, 25). A possible explanation is that different neuronal populations accumulate evidence for each decision, such that IPS acts as a dual accumulator during two-choice perceptual decisions. In the present experiment, participants made two-choice responses about whether a test probe was old or new. From a dual-accumulator view, IPS would be predicted to show HGP during both old and new decisions. By contrast, our data revealed that IPS was selectively active for recognized old items (Hits) up to 200 ms before the response, with activity during correctly identified new probes (CRs) remaining at baseline throughout the trial. This observation is consistent with recent fMRI findings and lesion data, suggesting that IPS selectively tracks the strength of evidence that an item is old (16, 22). Rather than supporting a dual-accumulator account of IPS function during old/new recognition, the present data suggest that IPS accumulates signed evidence toward a single bound that, when crossed, leads to an old response ∼200 ms later.

A possible explanation for the signed (single-bound) pattern of IPS activity is that participants may use a target detection decision strategy during old/new recognition, with old items as the target class. Although such a strategy is more likely when the ratio of old-to-new items is >1 (43, 44), it is possible that it is the default decision model when making old/new judgments. Interestingly, two fMRI studies suggest that IPS activity shows a Hits > CRs pattern independent of target class [i.e., independent of whether participants selectively respond to old items or to new items (45) or selectively indicate their confidence that a test probe is old or that a test probe is new (17)]. Although this might argue against IPS activity tracking the degree of evidence that a target is present, it remains possible, perhaps even highly plausible, that the psychologically natural target when making recognition memory decisions is always oldness. If this is the case, then participants may make an old item present/absent decision, and then map the decision to whatever the response rules are in the particular context.

Our data further demonstrate that increased HGP to Hits onsets in left IPS ∼300 ms poststimulus. Extant depth electrode recordings from human MTL have shown increased activity for hits as early as 200 ms poststimulus (46, 47). Although across-study comparisons are tenuous, the relative timing of these memory effects is compatible with a feed-forward signal propagating mnemonic evidence from MTL to IPS. Future studies that obtain simultaneous measures of MTL and parietal cortex activity promise to directly advance understanding of MTL–parietal retrieval dynamics and interactions.

A qualitatively distinct memory-related effect was observed in left SPL, wherein CRs elicited greater HGP than Hits. Left SPL activity, as measured with fMRI, has been observed to be greater for CRs than Hits (14). Moreover, recent fMRI data indicate that the left SPL regions implicated in goal-directed visual attention (30) are more active during uncertain memory decisions (11, 16, 17). The present pattern of SPL activity appears consistent with a top-down attention account. Specifically, the early increase in SPL HGP to CRs (200–300 ms poststimulus) suggests differential attention to novel retrieval probes, which is followed by comparable attention to old and new probes during the 300- to 700-ms window during which retrieval continues to unfold. Subsequently, there was a late (∼700 ms poststimulus onset) and sustained increase in SPL HGP to CRs, suggesting that differential attention is allocated during more uncertain decisions (RTs were longer for CRs than Hits) and persists through the response.

The decoding analyses provide a multivariate lens onto the spatial and temporal dynamics of recognition memory in left PPC. We note the numerical improvements in accuracy after including channels as features in the region-level decoding (e.g., stimulus-locked SPL across channels M = 54% vs. left SPL using channels M = 65% across participants), suggesting that there is complementary information across space within regions. When pooling IPS and SPL electrodes, we obtained mean accuracies of 65% and 70% for stimulus- and response-locked data, respectively. Interestingly, Hits vs. CRs classification accuracy did not improve from the single-region analyses. One possible account of this result

is that there is a common variable—mnemonic evidence—that drives the functional responses in these regions. In IPS, it takes the form of a mnemonic accumulator, and, in SPL, the absence of mnemonic evidence drives differential top-down attention to novelty and during the subsequent sustained search for mnemonic evidence. Future research with concurrent recordings from the MTL and PPC is needed to determine if IPS and SPL differentially track mnemonic evidence emerging from the MTL.

An important finding from the present study is that IPS and SPL showed distinct temporal patterns of activity for the two types of retrieval cues (old and new items). Specifically, after an initial novelty response 200 ms after trial onset, SPL responded to both Hits and CRs, and then showed a greater response later in the trial to CRs. By contrast, IPS demonstrated a selective response to Hits, with HGP for CRs not deviating from baseline; the IPS increase in HGP to Hits then fell to baseline ∼200 ms before participant's response. This temporal dissociation of dorsal parietal subregions runs counter to proposals that IPS and SPL are involved in similar processes during retrieval [e.g., goal-directed attention in service of retrieval (11)], and instead strongly favors a multiprocess functional organization in dorsal parietal cortex during memory-based decision making (14, 16).

We primarily focused on the high-frequency content (80–180 Hz) of the cortical surface LFP due to known correlations with local population activity (39–41) and the BOLD signal (35–38). We caution, however, that the relationship between these measures across the cortex is still a subject of debate in the field (48–50), and there also are other electrophysiological components that relate to memory. Concretely, scalp ERP analyses have demonstrated greater activity for source hits (recollected old items) over left parietal sites starting around 400 ms after cue onset (parietal old/new effect) (33). We performed ERP analyses by region and observed similar memory-related response profiles (*SI Text* and Figs. S11 and S12). Channel-wise analyses did not clearly differentiate between regions, with all three subregions (IPS, SPL, AG) showing Hits > CRs in either the 400- to 500-ms or the 500- to 600-ms window. Although future research is critically needed to address the source of the parietal old/new effect, our data provide an initial suggestion that multiple sources in left lateral parietal cortex may contribute to this effect.

Low-frequency bands of the LFP over parietal cortex also have been observed to vary with recognition memory. In particular, magnetoencephalography has revealed decreased low-frequency power for CRs compared with hits over left parietal cortex (51). We visualized possible low-frequency memory-related effects in left IPS and SPL using spectrograms to obtain finer time–frequency resolution (*SI Text* and Figs. S13 and S14). Corresponding analyses revealed a complex and nonmonotonic pattern of memory responses in the low-frequency ranges. Concretely, frequency bands below 30 Hz showed less power for CRs than Hits, with SPL channels showing the largest effect. This nontonal observation for low-frequency bands in ECoG data is commonly observed in the literature (52). Future research is needed to understand why the putative delta, theta, alpha, and beta bands, measured from left dorsal PPC, are not selectively involved in memory-guided decision making.

Collectively, the present data provide new evidence for a temporal cascade of memory-related activity across left dorsal PPC subregions, revealing the multifaceted nature of parietal function during memory-guided decisions. These data document a signed relationship between memory evidence and left IPS activity during decision making, and lend support for the role of SPL-mediated top-down attention during uncertain decisions. These observations inform models of the neurobiology of remembering, with implications for broader theories of parietal contributions to goal-directed behavior.

Materials and Methods

Participants. Eight male patients (mean age = 36.9 y; Table S1) diagnosed with refractory epilepsy participated after giving voluntary, informed written consent under an approved Stanford IRB protocol. Patients were implanted with strips and/or grids of intracranial electrodes, five patients with coverage in left PPC and three with coverage in right PPC (along with other sites; only parietal electrodes are reported here). Patients were implanted for clinical purposes related to the treatment of epilepsy; electrode placement was determined solely on clinical demands. Electrodes on or near a clinically identified seizure site were excluded from all analyses, as were electrodes that were clinically determined to show pathology.

Experimental Paradigm. The task protocol involved multiple rounds of study (encoding) and test (retrieval), with the exception of participant R3 (who had a single longer study–test round; see Table S1 and below). At encoding, participants made abstract/concrete decisions on a series of visually presented nouns. Participants were explicitly told that their memory for each word would be tested in the next round of the experiment. Each word was centrally presented (2.5 s), followed by a variable-duration intertrial interval (variable fixation cross; 1.5–3.5 s). Participants encoded 20 novel nouns in each study phase, and indicated their decisions by pressing one of two buttons using their right hand. Following encoding, participants rested for 1 min before starting the retrieval test. At retrieval, the 20 studied words were intermixed with 20 novel foils. Each test probe was centrally presented (1 s), followed by a maximum response period of 3.5 s. The intertrial interval randomly varied from 1.5 s to 3.5 s. For each test probe, participants could respond "high confidence old," "low confidence old," "low confidence new," or "high confidence new" by pressing one of four buttons with their right hand. Participants made few memory errors and provided few low-confidence responses (see Table S2); thus, analyses were constrained to only "high confidence old" responses to studied words (hits) and "high confidence new" responses to foils (CRs). Participant R3 received a longer version of the experiment, which consisted of a single study (160 words)/test (320 words) round. Stimulus presentation and participant response recording was conducted using PsychToolBox in MATLAB.

Data Recording. Electrocorticography was recorded using a multichannel system (Tucker-Davis Technologies). Data were recorded at 3,052 samples per second, band-pass filtered from 0.5 Hz to 300 Hz, and referenced to the most electrographically silent electrode. Data for participant L5 was recorded at half the sampling rate, with subsequent processing modified to match the other participants. A photodiode sensor on the stimulus presentation screen (sampled at 24.414 kHz) enabled accurate stimulus onset markers that were offline coregistered to the ECoG data.

Preprocessing. Data were digitally filtered offline from 1 Hz to 180 Hz using a Hanning window filter of length 1,000. Notch filters were applied at 60 Hz, and its first harmonic 120 Hz, to limit line noise. Data were down-sampled to 436 samples per second, and then rereferenced to the average of 10 channels with the lowest task response score (channels deemed clinically noisy or in one of the regions of interest—i.e., IPS, SPL, and AG—were not included in the rereference signal; see *SI Text* for details on how the 10 rereference channels were identified). This rereferencing procedure allowed us to investigate channels in IPS, SPL, and AG, while minimizing interregion contamination and the possibility that task-related effects in channels outside PPC would influence PPC channels. The referencing scheme had little effect on the HGP measures, as we obtained the same results using a common average. However, the referencing scheme did affect ERPs and lower frequency band power analyses.

Power Analyses. Using FIR filters, channels were filtered in the frequency band of interest: high gamma (80–180 Hz). The instantaneous amplitude of each band was obtained by taking the amplitude of the analytic signal, computed through the Hilbert transform. Subsequently, the signal was squared and transformed to a decibel scale to obtain an instantaneous power measurement. For each channel, the mean signal during each trial prestimulus window (200 ms) was subtracted to obtain trial-wise baseline correction. The nonparametric Mann–Whitney U test examined between-condition differences using the average signal from nonoverlapping 100-ms time bins, per channel; the U statistic was then converted to a Z statistic for across-channel analyses. The use of this nonparametric statistic allows us to make no assumptions about the distribution on the difference of condition means. Moreover, the resulting Z score is normally distributed across participants.

Univariate Statistics. Linear models were fitted to the memory scores (Z scores converted from U scores; Hits vs. CRs) to determine the significance of observed results. The critical contrast was the Region (IPS, SPL) × Time window (10 bins for stimulus-locked, 12 bins for the response-locked) interaction. An ANOVA table was constructed based on the fitted linear model, from which

the reported F statistics were obtained. The interaction (Region × Time) was subsequently unpacked when significant. To exclude the possibility of a single channel or participant driving the results, additional fixed-effects factors of Participant and Channel were included in the models.

Additionally, mixed-effects models were used to further validate the linear model results (see *SI Text*). In these models, we again tested the Region × Time interaction, with random effects given by Participant (intercept plus slopes of Time and Region) and Channel (intercept). Using a χ^2 statistic, the above model was evaluated against a reduced model that did not contain the interaction. Because, in this context (highly unbalanced data) the χ^2 statistic can be an unreliable estimate, we further computed the Kenward–Roger F Test approximation, which returns an F statistic with an approximate number of residual degrees of freedom. For the tests of memory effects in individual regions (IPS, SPL), the analogous mixed-effects model included a fixed-effect factor of Time, and random effects given by Participant (intercept) and Channel (intercept). Note that these models did not include a random slope term for Participant, as this set of models failed to converge when slope terms were included.

Clustering and Decoding Analyses. Please see *SI Text* for the full description of these analyses.

Code. Code is available online at https://github.com/WagnerLab/ECoG_PPC_RecogMemory.

ACKNOWLEDGMENTS. We thank Dr. Dora Hermes for cortex rendering code, Dr. Mohammad Dastjerdi for initial preprocessing scripts, and the Stanford Epilepsy Monitoring Unit Staff for assistance in data recording. This research was supported by National Institute of Neurological Disorders & Stroke (R01-NS078396), National Science Foundation (BCS-1358907), National Institutes of Health Biotechnology Training Grant (5T32GM008412-20 to A.G.), National Science Foundation Graduate Fellowships (to A.G. and K.F.L.), the Stanford Center for Mind, Brain, and Computation (A.G. and K.F.L.), and the Stanford NeuroVentures Program.

1. Squire LR (1992) Memory and the hippocampus: A synthesis from findings with rats, monkeys, and humans. *Psychol Rev* 99(2):195–231.
2. Cohen NJ, Eichenbaum H (2005) *Memory, Amnesia, and the Hippocampal System* (MIT Press, Cambridge, MA).
3. Shimamura AP (1995) Memory and the prefrontal cortex. *Ann N Y Acad Sci* 769: 151–159.
4. Eichenbaum H, Yonelinas AP, Ranganath C (2007) The medial temporal lobe and recognition memory. *Annu Rev Neurosci* 30(1):123–152.
5. Spaniol J, et al. (2009) Event-related fMRI studies of episodic encoding and retrieval: meta-analyses using activation likelihood estimation. *Neuropsychologia* 47(8-9): 1765–1779.
6. Rissman J, Wagner AD (2012) Distributed representations in memory: Insights from functional brain imaging. *Annu Rev Psychol* 63(1):101–128.
7. Buckner RL, Wheeler ME (2001) The cognitive neuroscience of remembering. *Nat Rev Neurosci* 2(9):624–634.
8. Carr VA, Rissman J, Wagner AD (2010) Imaging the human medial temporal lobe with high-resolution fMRI. *Neuron* 65(3):298–308.
9. Wagner AD, Shannon BJ, Kahn I, Buckner RL (2005) Parietal lobe contributions to episodic memory retrieval. *Trends Cogn Sci* 9(9):445–453.
10. Cabeza R (2008) Role of parietal regions in episodic memory retrieval: The dual attentional processes hypothesis. *Neuropsychologia* 46(7):1813–1827.
11. Cabeza R, Ciaramelli E, Olson IR, Moscovitch M (2008) The parietal cortex and episodic memory: An attentional account. *Nat Rev Neurosci* 9(8):613–625.
12. Vilberg KL, Rugg MD (2008) Memory retrieval and the parietal cortex: A review of evidence from a dual-process perspective. *Neuropsychologia* 46(7):1787–1799.
13. Hutchinson JB, Uncapher MR, Wagner AD (2009) Posterior parietal cortex and episodic retrieval: Convergent and divergent effects of attention and memory. *Learn Mem* 16(6):343–356.
14. Nelson SM, et al. (2010) A parcellation scheme for human left lateral parietal cortex. *Neuron* 67(1):156–170.
15. Yonelinas AP, Otten LJ, Shaw KN, Rugg MD (2005) Separating the brain regions involved in recollection and familiarity in recognition memory. *J Neurosci* 25(11):3002–3008.
16. Hutchinson JB, et al. (2014) Functional heterogeneity in posterior parietal cortex across attention and episodic memory retrieval. *Cereb Cortex* 24(1):49–66.
17. Hutchinson JB, Uncapher MR, Wagner AD (2015) Increased functional connectivity between dorsal posterior parietal and ventral occipitotemporal cortex during uncertain memory decisions. *Neurobiol Learn Mem* 117(C):71–83.
18. Olson IR, Berryhill M (2009) Some surprising findings on the involvement of the parietal lobe in human memory. *Neurobiol Learn Mem* 91(2):155–165.
19. Simons JS, Peers PV, Mazuz YS, Berryhill ME, Olson IR (2010) Dissociation between memory accuracy and memory confidence following bilateral parietal lesions. *Cereb Cortex* 20(2):479–485.
20. Berryhill ME, Phuong L, Picasso L, Cabeza R, Olson IR (2007) Parietal lobe and episodic memory: Bilateral damage causes impaired free recall of autobiographical memory. *J Neurosci* 27(52):14415–14423.
21. Davidson PSR, et al. (2008) Does lateral parietal cortex support episodic memory? Evidence from focal lesion patients. *Neuropsychologia* 46(7):1743–1755.
22. Hower KH, Wixted J, Berryhill ME, Olson IR (2014) Impaired perception of mnemonic oldness, but not mnemonic newness, after parietal lobe damage. *Neuropsychologia* 56:409–417.
23. Ben-Zvi S, Soroker N, Levy DA (2015) Parietal lesion effects on cued recall following pair associate learning. *Neuropsychologia* 73:176–194.
24. Tosoni A, Galati G, Romani GL, Corbetta M (2008) Sensory-motor mechanisms in human parietal cortex underlie arbitrary visual decisions. *Nat Neurosci* 11(12):1446–1453.
25. Heekeren HR, Marrett S, Ruff DA, Bandettini PA, Ungerleider LG (2006) Involvement of human left dorsolateral prefrontal cortex in perceptual decision making is independent of response modality. *Proc Natl Acad Sci USA* 103(26):10023–10028.
26. Heekeren HR, Marrett S, Ungerleider LG (2008) The neural systems that mediate human perceptual decision making. *Nat Rev Neurosci* 9(6):467–479.
27. Kiani R, Shadlen MN (2009) Representation of confidence associated with a decision by neurons in the parietal cortex. *Science* 324(5928):759–764.
28. Gold JI, Shadlen MN (2007) The neural basis of decision making. *Annu Rev Neurosci* 30(1):535–574.
29. Corbetta M, Shulman GL (2002) Control of goal-directed and stimulus-driven attention in the brain. *Nat Rev Neurosci* 3(3):201–215.
30. Corbetta M, Patel G, Shulman GL (2008) The reorienting system of the human brain: From environment to theory of mind. *Neuron* 58(3):306–324.
31. Ho TC, Brown S, Serences JT (2009) Domain general mechanisms of perceptual decision making in human cortex. *J Neurosci* 29(27):8675–8687.
32. Sestieri C, Corbetta M, Romani GL, Shulman GL (2011) Episodic memory retrieval, parietal cortex, and the default mode network: Functional and topographic analyses. *J Neurosci* 31(12):4407–4420.
33. Rugg MD, Curran T (2007) Event-related potentials and recognition memory. *Trends Cogn Sci* 11(6):251–257.
34. Hoppstädter M, Baeuchl C, Diener C, Flor H, Meyer P (2015) Simultaneous EEG-fMRI reveals brain networks underlying recognition memory ERP old/new effects. *Neuroimage* 116:112–122.
35. Niessing J, et al. (2005) Hemodynamic signals correlate tightly with synchronized gamma oscillations. *Science* 309(5736):948–951.
36. Mukamel R, et al. (2005) Coupling between neuronal firing, field potentials, and fMRI in human auditory cortex. *Science* 309(5736):951–954.
37. Engell AD, Huettel S, McCarthy G (2012) The fMRI BOLD signal tracks electrophysiological spectral perturbations, not event-related potentials. *Neuroimage* 59(3): 2600–2606.
38. Winawer J, et al. (2013) Asynchronous broadband signals are the principal source of the BOLD response in human visual cortex. *Curr Biol* 23(13):1145–1153.
39. Manning JR, Jacobs J, Fried I, Kahana MJ (2009) Broadband shifts in local field potential power spectra are correlated with single-neuron spiking in humans. *J Neurosci* 29(43):13613–13620.
40. Liu J, Newsome WT (2006) Local field potential in cortical area MT: Stimulus tuning and behavioral correlations. *J Neurosci* 26(30):7779–7790.
41. Katzner S, et al. (2009) Local origin of field potentials in visual cortex. *Neuron* 61(1): 35–41.
42. Kahn I, Davachi L, Wagner AD (2004) Functional-neuroanatomic correlates of recollection: Implications for models of recognition memory. *J Neurosci* 24(17):4172–4180.
43. Herron JE, Henson RNA, Rugg MD (2004) Probability effects on the neural correlates of retrieval success: An fMRI study. *Neuroimage* 21(1):302–310.
44. Vilberg KL, Rugg MD (2009) An investigation of the effects of relative probability of old and new test items on the neural correlates of successful and unsuccessful source memory. *Neuroimage* 45(2):562–571.
45. Shannon BJ, Buckner RL (2004) Functional-anatomic correlates of memory retrieval that suggest nontraditional processing roles for multiple distinct regions within posterior parietal cortex. *J Neurosci* 24(45):10084–10092.
46. Mormann F, et al. (2005) Phase/amplitude reset and theta-gamma interaction in the human medial temporal lobe during a continuous word recognition memory task. *Hippocampus* 15(7):890–900.
47. Staresina BP, Fell J, Do Lam ATA, Axmacher N, Henson RN (2012) Memory signals are temporally dissociated in and across human hippocampus and perirhinal cortex. *Nat Neurosci* 15(8):1167–1173.
48. Buzsáki G, Anastassiou CA, Koch C (2012) The origin of extracellular fields and currents—EEG, ECoG, LFP and spikes. *Nat Rev Neurosci* 13(6):407–420.
49. Ekstrom A (2010) How and when the fMRI BOLD signal relates to underlying neural activity: The danger in dissociation. *Brain Res Brain Res Rev* 62(2):233–244.
50. Conner CR, Ellmore TM, Pieters TA, DiSano MA, Tandon N (2011) Variability of the relationship between electrophysiology and BOLD-fMRI across cortical regions in humans. *J Neurosci* 31(36):12855–12865.
51. Osipova D, et al. (2006) Theta and gamma oscillations predict encoding and retrieval of declarative memory. *J Neurosci* 26(28):7523–7531.
52. Burke JF, Ramayya AG, Kahana MJ (2015) Human intracranial high-frequency activity during memory processing: Neural oscillations or stochastic volatility? *Curr Opin Neurobiol* 31:104–110.
53. Hermes D, Miller KJ, Noordmans HJ, Vansteensel MJ, Ramsey NF (2010) Automated electrocorticographic electrode localization on individually rendered brain surfaces. *J Neurosci Methods* 185(2):293–298.
54. Dalal SS, et al. (2008) Localization of neurosurgically implanted electrodes via photograph-MRI-radiograph coregistration. *J Neurosci Methods* 174(1):106–115.